Thermo-physical characteristics of 3C-SiC structure subjected to microwave exposure: A molecular dynamics study

T L Dora[1], Ayush Owhal[1], Tribeni Roy[1, 2], Sachin U Belgamwar[1], Saurav Goel[2, 3], Hamed Yazdani Nezhad[4], Radha Raman Mishra[1, 4*]

[1]Department of Mechanical Engineering, Birla Institute of Technology and Science Pilani, Pilani-333031, India.

[2]School of Engineering, London South Bank University, London, SE10AA, United Kingdom

[3]University of Petroleum and Energy Studies, Dehradun, 248007, India.

[4]Department of Mechanical Engineering & Aeronautics, School of Science and Technology, City University of London, London EC1V 0HB, United Kingdom.

* Corresponding authors:

rraman.mishra@pilani.bits-pilani.ac.in (First corresponding author)

Hamed.Yazdani@city.ac.uk (Second corresponding author)

Highlights

- Microwave heating of bulk 3C-SiC have been studied using MD simulations
- Rapid microwave heating was observed at 0.5 V/Å and 500 GHz
- Increase in diffusion coefficient changes physical phase of the 3C-SiC system
- Physical state of the system changed by 75% relative to initial structure with in 5ns

Abstract

Silicon carbide (SiC) is widely used as a susceptor for microwave hybrid heating applications owing to its exceptional microwave absorbing characteristics. In practice, it is challenging to characterize the thermo-physical behaviour of the microwave irradiated SiC-based targets experimentally due to interference of integrated measurement devices with microwaves. In this article, molecular dynamics simulations were performed to understand the atomistic response of a bulk 3C-SiC model during microwave heating. Atomistic simulations were performed at different electric field strengths (ranging from 0.1 to 0.5 V/Å) and frequencies (ranging from 100 to 500 GHz) to develop a numerical relationship between temperature and time in order to predict the thermal response of bulk 3C-SiC. On the other hand, the physical characteristics of the bulk 3C-SiC were determined by the plots between mean square displacement (MSD), time and diffusion coefficients. The results showed that at 0.5 V/Å electric field strength and 500 GHz frequency, the diffusion coefficient increased up to 88% as compared to the electric field strength of 0.1 V/Å at 500 GHz. A change of 75% in the physical phase of 3C-SiC structure with respect to the initial structure was confirmed by the distorted density distribution profile.

Keywords: Microwave heating, molecular dynamics, 3C-SiC, electric field strength, frequency, atomistic simulation

1. Introduction

Microwave (MW) energy has been exploited for processing of various engineering materials such as polymers, ceramics, metals and alloys, and their composites [1–4]. Processing of materials that are transparent to microwaves (e.g., alumina) or reflect microwaves (e.g., bulk metals) at room temperature is challenging as result of minimal dissipation of microwave energy inside these materials due to limited and uneven depth of penetration driven by dissimilar absorption properties [1,5–8]. Additionally, microwave absorbing materials are sometimes impacted by thermal runaway that are caused due to the development of hot spots during direct microwave heating [1,3,7,9,10]. In order to overcome these challenges, Microwave Hybrid Heating (MHH) approach has largely been used to process these materials to achieve improved properties in the developed parts [1–3,7,9–14]. In MHH, heating of the target material is accomplished using conventional and microwave heating approaches. Firstly, a susceptor which is a microwave absorbing material such as SiC absorbs microwave energy and heats the target material (conventional heating) till it attains the material specific critical temperature [1,3,12,15]. Beyond, its critical temperature, it starts absorbing microwave energy (microwave heating). Most widely used susceptor material in MHH is SiC. It is, therefore, understanding of the physics behind the microwave-material interaction that causes heat dissipation inside the susceptor material during MHH plays a vital role in selection of the susceptor material. Any experimental investigation has not been reported on any material to

study the heat dissipation phenomena at atomic level due to the limited experimental resources; however, few simulation studies have been reported on materials such as water [16], monoethanolamine (MEA) [17], polyacrylonitrile (PAN) [18], supercritical water [19] and alumina (α-Al_2O_3) [20] based on Molecular Dynamics (MD) simulation. To study the modeling and simulation of different materials such as metal, ceramics, polymers, oxides, etc., at the molecular level, classical molecular dynamics (MD) has emerged as a viable technique [21,22]. Large-scale Atomic/Molecular Massively Parallel Simulator (LAMMPS) is an open-source and classical MD tool has been popularly used for simulation work [23]. Dielectric response of the liquid water was studied at different microwave frequencies using eight empirical force fields [16]. It was reported that TIP4P-ε and OPC3 force field was the most efficient in accurately predicting the dielectric spectra of liquid water. In another study, the dielectric heating of liquid monoethanolamine (MEA) was analyzed at different MW frequencies (1.0-10.0 GHz) by using the force fields GROMOS-aa that effectively predicted the dielectric characteristics of MEA [17]. Further, analysis of microwave heating of polyacrylonitrile (PAN) was reported using a reactive force field and it was revealed by the study that temperature change in PAN was dependent on applied EM field strength and frequency [18]. Microwave heating characteristics of supercritical water was studied in terms of fast MW heating and associated energy distribution by predicting the mean square displacement (MSD) and diffusion coefficient [19]. The applied MW energy was stored as inter molecular energy (40%) which rearrange molecules and the system gets heated at a higher rate (75%). Further, microwave heating characteristics of ceramic materials such as α–Al_2O_3 [20] and SiC [24] were also reported. The α–Al_2O_3 was analyzed using a non-equilibrium MD simulation and the study revealed that microwave heating characteristics of α–Al_2O_3 depends upon alignment of various crystallographic directions with applied electric field [20]. In another study, heating of silicon carbide (SiC) was analyzed under microwave irradiation [24]. It was reported that rise in temperature of SiC was substantially faster when microwaves were applied parallel to SiC surface <100>; whereas, lesser heating of SiC slab was predicted in a perpendicular direction to the SiC surface. It is evident from the relevant literature that thermo-physical characteristics of SiC which provides useful information to utilize SiC as susceptor in MHH of different materials has not been studied using MD simulations. Therefore, in the present paper, rapid microwave heating of silicon carbide (3C-SiC) was studied at different frequencies (100, 200, 300, 400 and 500 GHz) and electric field strengths (0.1, 0.2, 0.3, 0.4 and 0.5 V/Å). Microwave heating characteristics of 3C-SiC was analyzed using the mean square displacement and the diffusion coefficient. Finally, phase change in SiC was predicted during microwave exposure.

2. Materials and Methods

The bulk SiC system, cubic zinc-blend structure (3C-SiC), with periodic boundaries in the x, y, and z directions was used to perform the simulation study. The lattice constant of the bulk 3C-SiC was taken as 4.35 Å [25] and the cubic cell size was 34.8 Å in each direction. Fig. 1 schematically illustrates the original atomic arrangement, size of the bulk SiC, and direction of propagation of microwaves (*x*-direction).

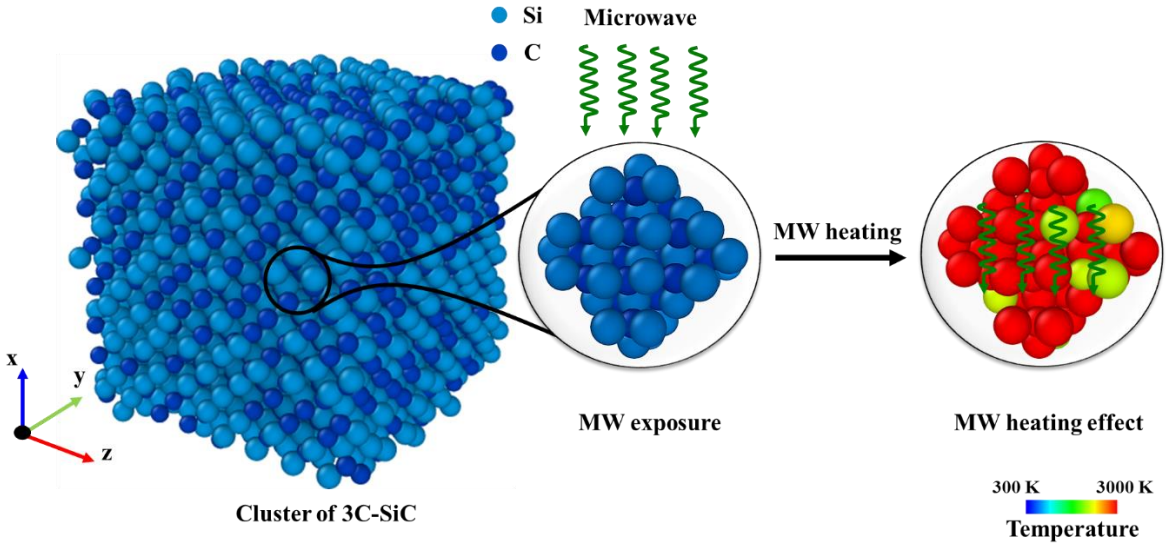

Fig. 1. A schematic representation of atomistic model of the bulk 3C-SiC (4096 atoms) and microwave heating (insert) using Vashishta force field.

Vashishta's interatomic potential offers accurate prediction of dislocation behavior [26], diffusion behavior [27], temperature evolution in microwave heating [24] while analyzing 3C-SiC system. Therefore, Vashishta potential was used for this study to illustrate the pair-wise interaction between the atoms [28,29]. Vashishta force field comprises two- and three-body interactions. The total potential energy (PE) of a system can be represented by Eq. 1 [28,30] –

$$U = \sum_i^N \sum_{i<j}^N U_{ij}^{(2)}(r_{ij}) + \sum_i^N \sum_{j\neq i}^N \sum_{j<K,k\neq i}^N U_{ijk}^{(3)}(r_{ij}, r_{ik}, \theta_{ijk}). \quad (1)$$

where, the term U is the effective interatomic potential, $U_{ij}^{(2)}(r_{ij})$ indicates two-body interaction potential, and $U_{jik}^{(3)}(r_{ij}, r_{ik}, \theta_{ijk})$ indicates three-body interaction potential of a system. The steric size effects of the ions, charge-transfer mechanisms leading to Coulomb interactions, charge-dipole interactions owing to the electronic polarizability of ions, and induced dipole-dipole (van der Waals) interactions are part of the two-body interaction potential which is represented as [28,30]-

$$U_{ij}^{(2)}(r) = \frac{H_{ij}}{r^{\eta_{ij}}} + \frac{Z_i Z_j}{r} e^{-r/\lambda} - \frac{D_{ij}}{2r^4} e^{-r/\xi} - \frac{W_{ij}}{r^6}. \quad (2)$$

where, H_{ij} is the strength of the steric repulsion, $Z_{i,j}$ is the effective charge, D_{ij} is the strength of the charge-dipole attraction, W_{ij} is the van der Waals interaction strength, η_{ij} is the exponents of the steric repulsion term, $r \equiv r_{ij}$ is the distance between the *i*th atom at position r_i and the *j*th atom at position r_j, λ is the screening lengths for Coulomb term, and ξ is the

screening lengths for charge-dipole term. The three-body part of the effective potential is represented by Eq. 2 [28,30] -

$$U_{ijk}^{(3)}(r_{ij}, r_{ik,}\theta_{ijk}) = B_{ijk} exp\left(\frac{\gamma_{ij}}{r_{ij}-r_0} + \frac{\gamma_{ik}}{r_{ik}-r_0}\right) \frac{[\cos\theta_{ijk} - \cos\bar{\theta}_{ijk}]^2}{1+C_{ijk}[cos\,\theta_{ijk} - cos\,\bar{\theta}_{ijk}]^2}. \quad (3)$$

where, B_{ijk} is the strength of interaction, θ_{ijk} is the angle formed by r_{ij} and $r_{ik,}C_{ijk}, and\ \underline{\theta}_{ijk}$ is a constant.

In the present study, LAMMPS was used as a MD tool and OVITO platform was used to visualize atoms and molecular movements as well as to accomplish the post-processing of the MD simulation. Simulation of microwave heating of the bulk 3C-SiC was carried at different electric field strength (0.1, 0.2, 0.3, 0.4 and 0.5 V/Å) and the frequencies (100, 200, 300, 400 and 500 GHz). Initially, equilibration of all the systems was done in a canonical (NVT) ensemble using the Nose-Hoover thermostat [31] for 2.5 ns. Simulation in each case was equilibrated to room temperature with a temperature damping factor of 0.1 ps. These atomistic configurations were used finally to accomplish the targeted studies. The bulk 3C-SiC system is a non-magnetic system; therefore, it gets affected by the electric field component of the microwave energy [32]. An external alternating electric field was, thus, applied in *x*-direction within a micro-canonical (NVE) ensemble utilizing the velocity-Verlet algorithm [16,18–20] to analyze the effect of microwave on the bulk 3C-SiC system. The external alternating electric field caused by microwave exposure can be expressed as [16,20] -

$$E(t) = E_n sin\,(2\pi f t). \quad (4)$$

where, $\mathbf{E_n}$ is electric field strength or the amplitude, *f* is the frequency, and *t* is the elapsed time for microwave exposure. The bulk 3C-SiC system was exposed to microwaves for 5 ns during the simulation study. The external electric field adds a force (i.e., **F**=q**E**) to each charged atom in the system. Calculation of Coulomb interaction for microwave induced dipole moments in microwave exposed 3C-SiC system is vital. Therefore, the charge assigned to Silicon (Si) and Carbon (C) were 1.201 and -1.201, respectively, as per Vashishta's interatomic potential [24]. The outcomes of the simulation study have been discussed in subsequent section.

The bulk 3C-SiC system was equilibrated at a constant volume and temperature (NVT) ensemble for 2.5 ns with timestep 0.001 ps. An initial velocity was provided to the system to achieve a temperature of 298 K [17,20]. Fig. 2 indicates variation of temperature and potential energy before and after the equilibration stage with respect to time. After providing some random initial velocity in an NVT ensemble, the temperature and potential energy of the system increases up to 1 ns (Fig. 2) and gets stabilized to constant values approximately 298 K and -25800 eV, respectively. Subsequently, the equilibrated system was utilized to simulate the influence of varying electric field strength and frequency on microwave heating behavior and thermo-physical characteristic of the 3C-SiC system.

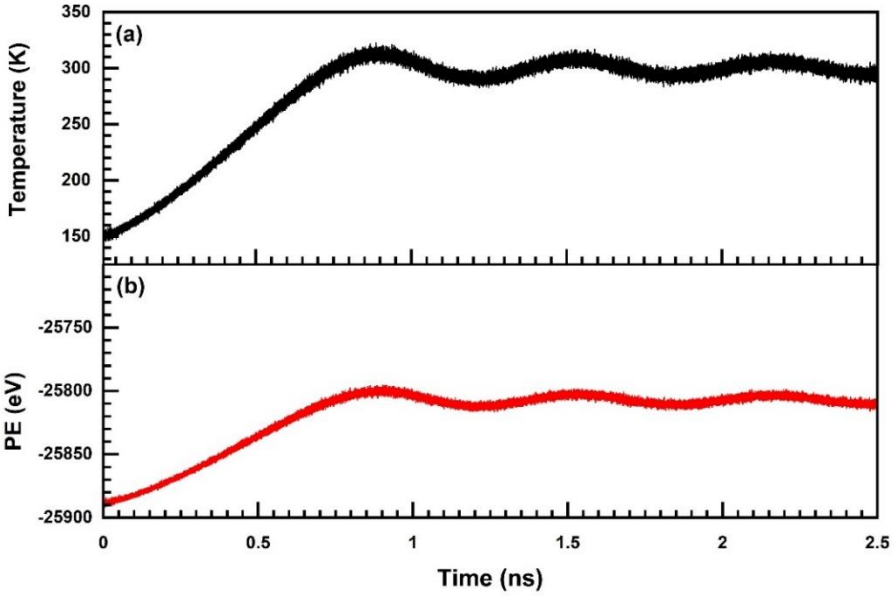

Fig. 2. Temperature and potential energy variation with time after equilibration of 3C-SiC system. The equilibration was performed in an NVT ensemble at a temperature of 298K for 2.5 ns.

A non-strict NVE ensemble was used to consider the microwave energy absorption in the 3C-SiC system during microwave exposure [33]. Initially, the bulk 3C-SiC system was simulated without applying external electric field (**E**=0). Subsequently, the bulk 3C-SiC system was exposed to microwaves at different frequencies (*f*) 100, 200, 300, 400 and 500 GHz and simulations were carried out at electric field strengths ($\mathbf{E_n}$) varying from 0.1, 0.2, 0.3, 0.4 and 0.5 V/Å. Accordingly, the obtained results have been discussed in the following section.

3. Results and discussions

Fig. 3 depicts the temperature and kinetic energy (KE) profile of a bulk 3C-SiC system in an NVE ensemble without the introduction of any external electric field (**E**=0). No considerable increase in temperature and KE in the NVE ensemble (Fig. 3) confirms that the initial configuration used for the MD simulations is very well equilibrated. Therefore, any surge in temperature and kinetic energy may be attributed to the possibility of the system being exposed to an external electric field [16].

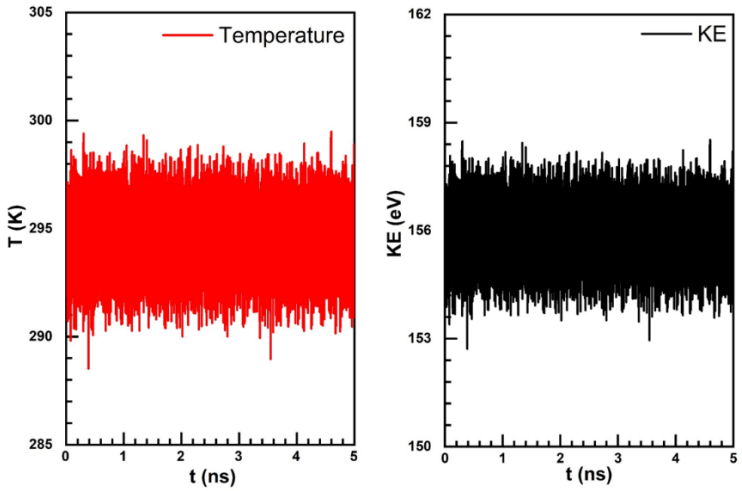

Fig. 3. Variation of temperature (*T*) and Kinetic energy (KE) with time in an NVE ensemble without any external electric field (**E** = 0)

Fig. 4 shows the temperature profiles of the microwave irradiated bulk 3C-SiC system with increase in time at different *f* and different $\mathbf{E_n}$ values of a time-dependent external electric field. It was evident from Fig. 4 that temperature rises when an external electric field was introduced to the system. Moreover, temperature increases as frequency increases from 100 to 500 GHz. Microwave exposed bulk 3C-SiC system attains melting temperature (3300 K[34]) in 5 ns at 500 GHz and 0.5 V/Å. Therefore, further analysis has been carried out at a frequency of 500 GHz and electric field strength of 0.1 to 0.5 V/Å.

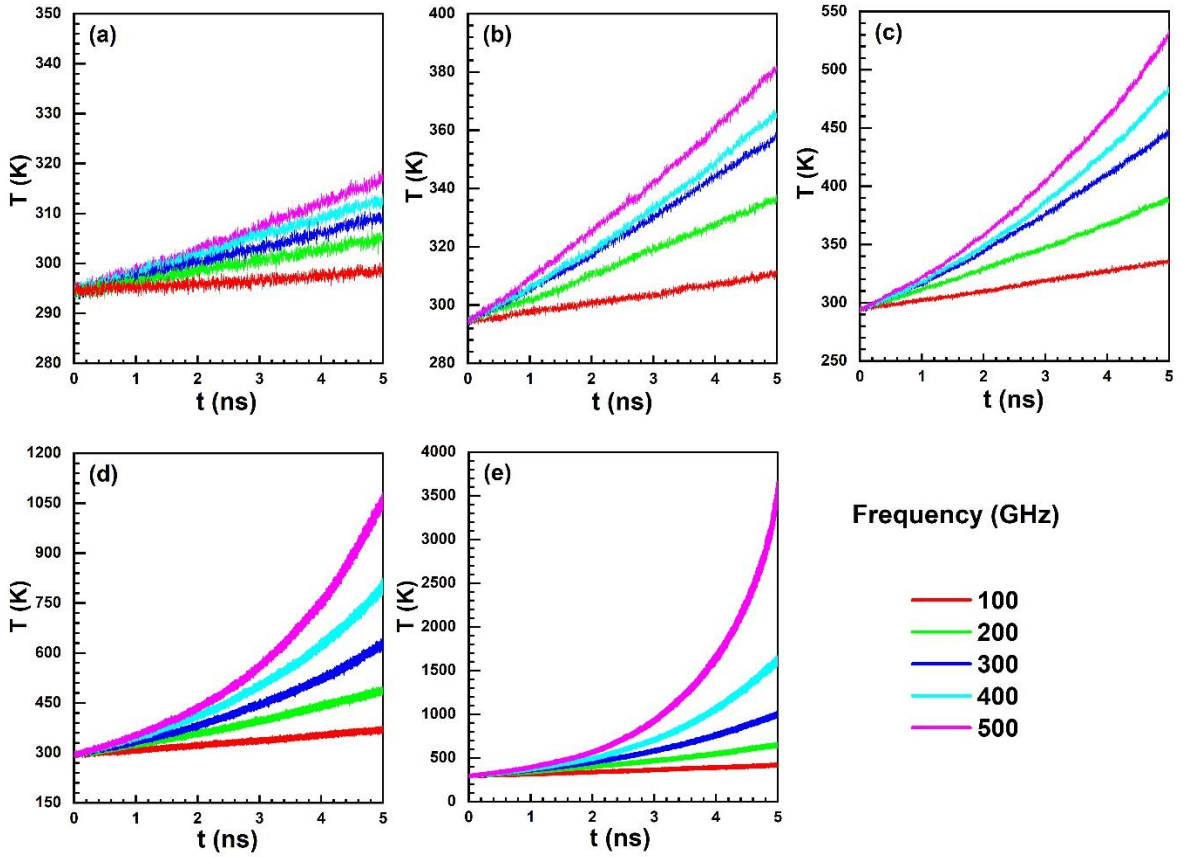

Fig. 4. Variation of temperature (*T*) at different frequencies with time (*t*) during microwave exposure of the 3C-SiC at different **E** field strength (a) 0.1 V/Å, (b) 0.2 V/Å, (c) 0.3 V/Å, (d) 0.4 V/Å, and (e) 0.5 V/Å

It can be observed that increase in electric field strength enhances the temperature of the system at a constant frequency; for example, temperature increase up to 1063% in 5 ns while changing $\mathbf{E_n}$ from 0.1 to 0.5 V/Å at 500 GHz (Fig. 4a-e). Additionally, the system attains a temperature of 1100 K in 20% shorter duration when electric field strength was changed from 0.4 V/Å to 0.5 V/Å at frequency 500 GHz (Fig. 4d-e). The observed increase in temperature at higher external electric field (0.5 V/Å) and frequency (500 GHz) can be attributed to the higher dissipation of heat in the SiC due to higher displacement of dipoles from their mean position and increased number of oscillation cycles per unit time [1, 3]. Rapid heating of the SiC system can be observed beyond 2.5 ns at 0.5 V/Å and 500 GHz and attains melting temperature (3100 ± 40 K [34]) within 4.87 ns (Fig. 4e). It has been reported by Aissa et al. that rapid microwave

heating of the SiC up to 2000 K occurs at 900 W and 2.45 GHz within 100s [35]. The observed variation in heating time reported in the previous work and the present work is due to the variation in external electric field strength and frequency.

It is apparent from the above discussion that microwave heating of the bulk 3C-SiC system was significantly influenced by the microwave frequency and electric field strength and the temperature varies non-linearly with time at different microwave frequencies and electric field intensities (Fig. 4). It is noteworthy, while curve fitting of the temperature-time characteristics (Fig. 4) of the bulk 3C-SiC system that temperature rises exponentially with respect to time and it can be represented mathematically as [18,36] -

$$T(t) = T_0 \times e^{(\beta t)}. \quad (5)$$

where, T is the system temperature in K, T_0 is the initial temperature of the system in K, t is the simulation time in ns and β is the correlation coefficient.

Fig. 5a illustrates the 3D heating profile of the bulk 3C-SiC system with respect to the obtained β values, electric field strengths, and frequencies. The correlation coefficient β for all the 25 cases have been estimated and surface fitting of the contours provides a cumulative Gaussian function (R^2 = 0.994) that adequately describes the correlation between β, $\mathbf{E_n}$ and f. The exponential fit of temperature profile of the bulk 3C-SiC system at 0.5 V/Å and 500 GHz is shown in Fig. 5b. The correlation coefficient (β) and coefficient of determination for this case were estimated as 4.53×10^{-7} and 0.951, respectively during the exponential fit of temperature-time profile.

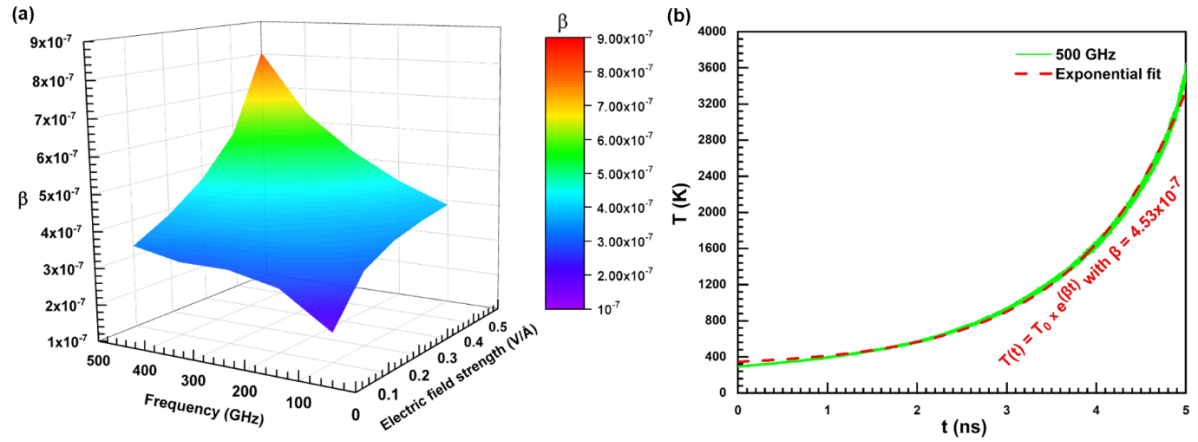

Fig. 5 (a). Variation of 3D heating profile (surface fit) of correlation coefficient (β) with **E** field strengths and frequencies for bulk 3C-SiC system, and (b). Temperature-time plot at 0.5 V/Å and 500 GHz.

The cumulative Gaussian function surface fit was applied to the β values and a numerical relationship between the β and input microwave parameters was established for quantitative estimation of the degree by which β was influenced by electric field strength and frequency. The numerical relationship between β, f, and **E** field strength can be represented by the following equation [18,24,36] -

$$\beta = A_0 + 0.25\, B_0 \times \left[1 + erf\left\{\frac{\boldsymbol{E_n}(V/Å) - C_0}{\sqrt{2}D_0}\right\}\right] \times \left[1 + erf\left\{\frac{f(GHz) - E_0}{\sqrt{2}F_0}\right\}\right]. \quad (6)$$

where, the terms A_0, B_0, C_0, D_0, E_0 and F_0 are the fitting parameters and $\mathbf{E_n}$ and f are the microwave electric field strength and frequency, respectively. The values of fitting parameters estimated for cumulative Gaussian function of β are listed in Table 1.

Table. 1 The values of fitting parameters for β

Fitting parameters	**Values**
A_0	$7.93\times10^{-9} \pm 5.374\times10^{-9}$
B_0	$1.89\times10^{-6} \pm 9.704\times10^{-7}$
C_0	0.59 ± 0.11
D_0	0.21 ± 0.04
E_0	381.20 ± 47.88
F_0	245.71 ± 32.81

Consequently, equations (5) and (6) can be used to explain the microwave heating characteristics of the bulk 3C-SiC at different electric field strengths and frequencies using MD simulations over a suitable simulation period.

Fig. 6 shows the variation in kinetic energy (KE) of the bulk 3C-SiC with microwave exposure time at different frequencies and electric field strengths. It confirmed that the rise in temperature of the system was driven by the applied microwave field which caused increase in the KE of the atoms. The microwaves interact with atoms of the system and transfers wave energy to atoms of the 3C-SiC system; as a result, the KE of the system increases [19,20]. The KE gained by the atoms during microwave interaction is directly proportional to $\mathbf{E_n}$ and f of the microwaves; consequently, the KE of the system increases [20]. It was evident from Fig. 6 that increase in $\mathbf{E_n}$ (0.1, 0.2, 0.3, 0.4, and 0.5 V/Å) or f (100, 200, 300, 400 and 500 GHz) values, increases the KE within the system. Significant increase in the KE of the system was apparent at electric field strengths of 0.5 V/Å and frequency of 500 GHz (Fig. 6e). The rise in the KE of atoms of the system results in various losses associated with inertia, elastic, frictional and molecular interaction forces in the system and causes increase in the system temperature which is shown in Fig. 4. In general, change in electric field strengths and frequencies causes change in positions of the atoms of SiC molecules significantly [37]. Therefore, molecular collisions in the bulk 3C-SiC system affects the structural and thermal stability of the system at every time step of microwave heating [38].

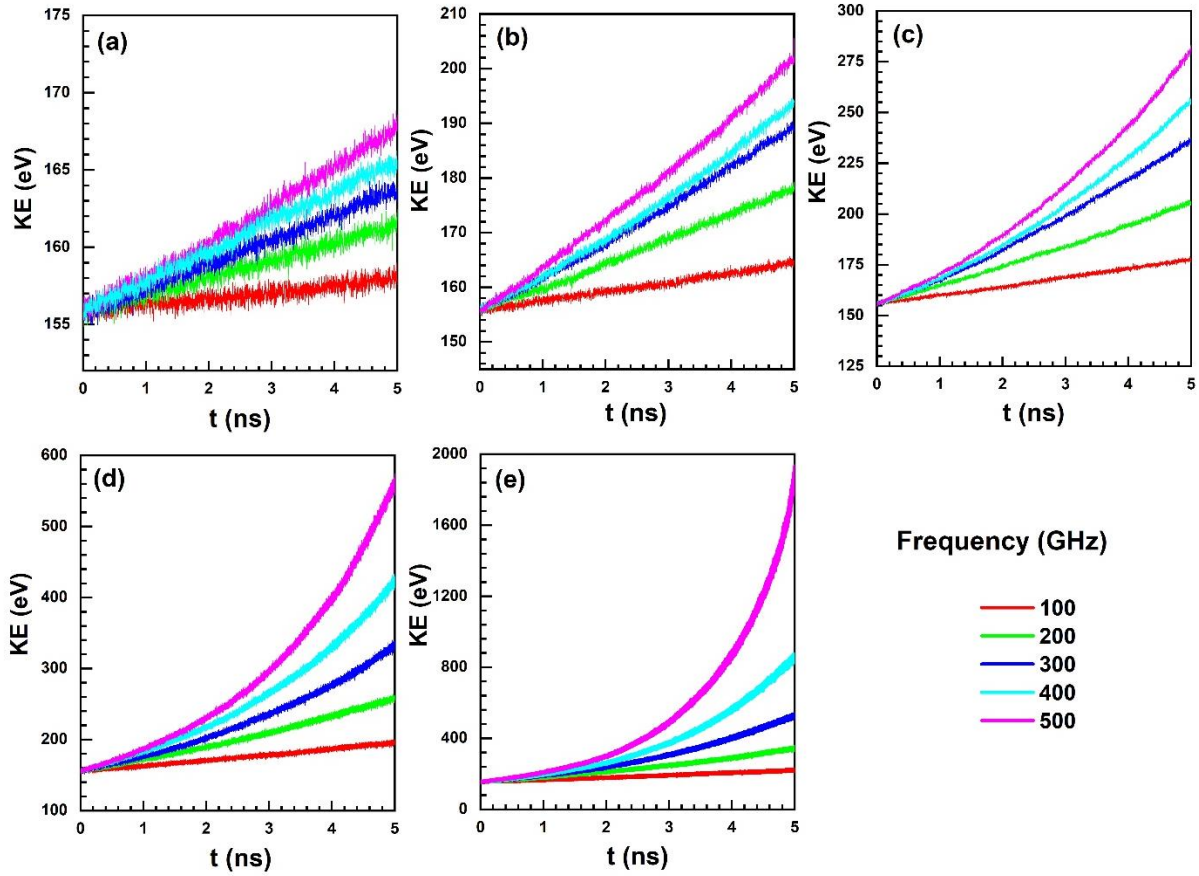

Fig. 6. Variation KE of the bulk 3C-SiC system with time during microwave exposure at different electric field strengths (a) 0.1 V/Å, (b) 0.2 V/Å, (c) 0.3 V/Å, (d) 0.4 V/Å, and (e) 0.5 V/Å.

Particle mobility can be assessed using the mean square displacement (MSD) which is an average of the square of particle displacements [39–41]. The MSD of a system can be calculated using the below equation [42–44] -

$$\overline{MSD}(t) = \frac{1}{N}\sum_{i=1}^{N}|r_i(t) - r_i(0)|^2 \quad (8)$$

where, $r_i(t)$ and $r_i(0)$ is the atom position of the i^{th} atom after t time of simulation and t =0 respectively and N is the number of atomic sites. Variation of MSD of the system with time is shown in Fig. 7 at different $\mathbf{E_n}$ values and 500 GHz. It is indicated by the plots (Fig. 7) that the MSD values for the system increases at a higher rate with increase in the electric field strength. Increase in MSD values with time was approximately linear for an initial 2 ns during microwave exposure (Fig. 7, insert). The derivative of MSD represents the diffusivity of system and it has been frequently used to determine the dynamic properties of system [38,39]. The diffusion coefficient (D) of atoms can be estimated by the slope of MSD-time plot with respect to time ($t = t_1 - t_0$; where t is time interval between some given time t_1 and initial time t_0) using the below equation [38,45–47],

$$D = \frac{1}{6t}\langle MSD(t_1) - MSD(t_0)\rangle \quad (9)$$

The values of diffusion coefficient (D) were calculated at 500 GHz by varying the electric field strengths (0.1, 0.2, 0.3, 0.4, 0.5 (Phase I) and 0.5 (Phase II) V/Å).

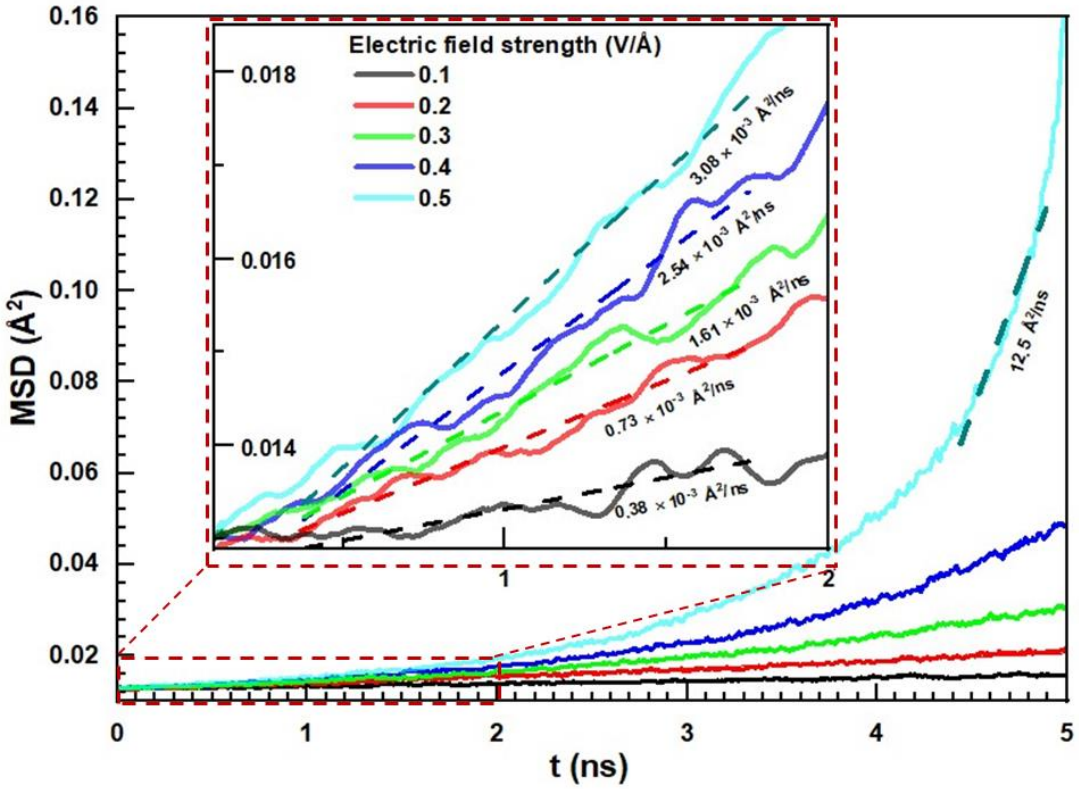

Fig. 7. Variation of MSD of the 3C-SiC system with time at different electric field strengths and at 500 GHz frequency. (Insert shows the variation of MSD for initial 2 ns).

The variation of diffusion coefficient with electric field strength is shown in Fig. 8. For electric field strength 0.1 V/Å, the calculated slope of MSD curve is 0.38×10^{-3} Å^2/ns (Fig. 7) and it provides the diffusion coefficient of 0.633×10^{-4} Å^2/ns which is the lowest among all heating cases (Fig. 8).

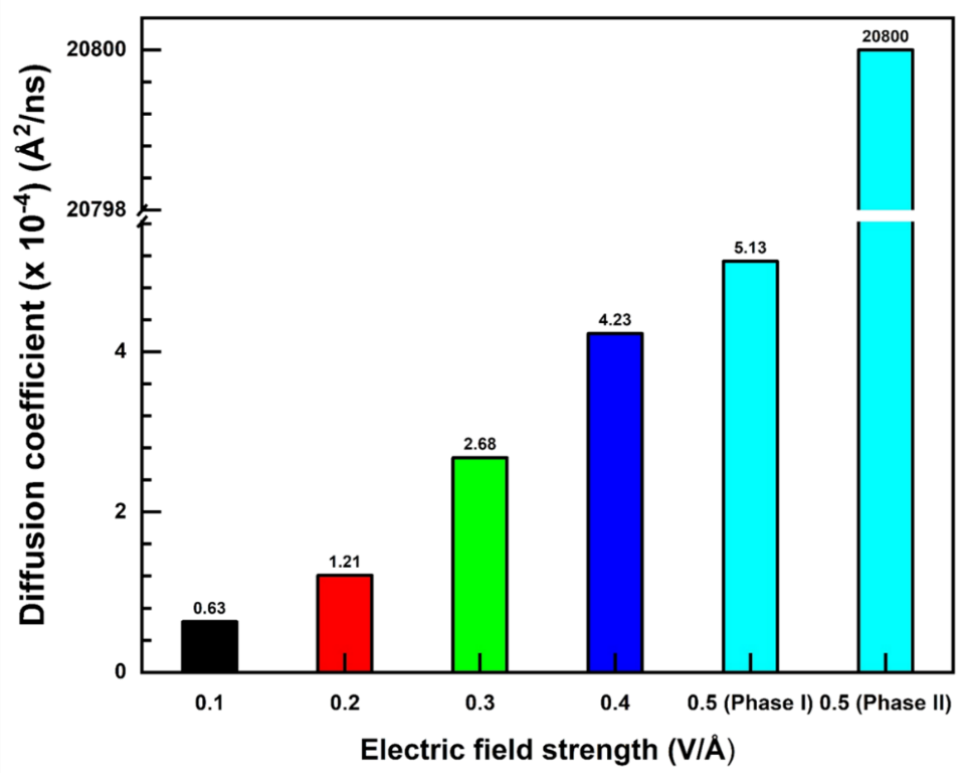

Fig. 8. Diffusion coefficient of 3C-SiC model for different **E** field strengths at 500 GHz frequency during MW heating. Here, at **E** field strength of 0.5 V/Å, phase I and II represents diffusion coefficient before and after 2 ns of simulation time.

The slope of the MSD curve up to 2 ns (Fig. 7, Phase-I) at 0.5 V/Å is 3.08×10^{-3} Å^2/ns and the corresponding estimated diffusion coefficient is 5.11×10^{-4} Å^2/ns, which is 87.66 % higher than the heating condition of electric field strength of 0.1 V/Å at 500 GHz frequency. After 2 ns of heating at 0.5 V/Å and 500 GHz, the slope of the MSD curve (Fig. 7, Phase-II) increases exponentially and approaches a value of 12.5 Å^2/ns; accordingly, the diffusion coefficient is estimated 2.08 Å^2/ns which is the highest among all heating cases (Fig. 8). Generally, a change of solid phase of the 3C-SiC structure to a liquid phase occurs up to 2.08 Å^2/ns [38]. Therefore, to understand the change in an atomistic arrangement of the 3C-SiC structure during microwave heating, the temporal density profile distributions of the 3C-SiC system were plotted at 0.5 V/Å and 500 GHz and the generated plot is shown in Fig. 9.

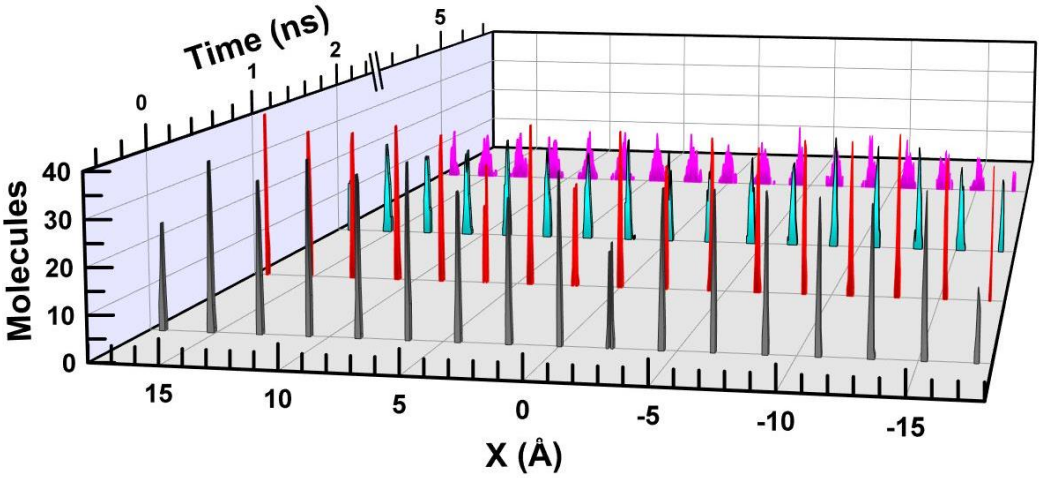

Fig. 9. Temporal density distribution profile of 3C-SiC molecules along *x*-direction at **E** field strength 0.5 V/Å and frequency 500 GHz.

It is apparent from Fig. 9 that microwave exposure of the 3C-SiC up to 5 ns at 0.5 V/Å and 500 GHz distorts crystallographic arrangement of the 3C-SiC system by broadening the density peaks, whereas the density peaks were nearly well arranged up to 2 ns of microwave exposure.

Table. 2. Number of molecules at specific distances at different time

Distance (Å)	**No. of molecules in Time (ns)**			
	0	**1**	**2**	**5**
-15	36	33	22	10
-10	34	37	27	15
-5	35	35	21	12
0	38	38	24	12
5	33	39	23	15
10	39	38	23	12
15	38	36	24	13

Number of molecules present at specific distance -15, -10, -5, 0, 5, 10 and 15 during MW exposure to the 3C-SiC system at different time intervals 0, 1, 2 and 5 ns are presented in Table

2. With reference to the initial configuration, the total number of molecules decreased by around 75% during MW heating at 5 ns for all indicated distance (Table 2). It is in good agreement with the higher value of diffusivity for microwave exposed 3C-SiC system at 0.5 V/Å and 500 GHz (Fig. 8) and exponential change in phase of diffusion coefficient values.

In the present study, although a high electric field strength of 0.5 V/Å at 500 GHz frequency is used in the MD simulation of 3C-SiC, the observed rapid heating of 3C-SiC in simulation results eventually aligns with the experimental observations reported by researchers while heating of 3C-SiC [48,49]. The relevant literature demonstrates that the experimental studies reported for microwave heating of materials are mostly limited to monitoring of the temperature, post-experimental observations for assessment of the microwave heating effects on material. On the other hand, the presented study provides valuable insights into the rapid heating phenomena at atomic level, i.e., structural changes in SiC due to conversion of SiC from the solid phase to the liquid phase. Moreover, it is usual to use high electric field strength and frequency for microwave heating of materials during MD simulation [20,24,33]. This approach is generally practical to overcome the limitations of current computational resources.

4. Conclusions

In the present work, simulation of microwave heating of 3C-SiC system was carried out using molecular dynamics simulation at different electric field strengths and frequencies. The following can be concluded from the study –

- Rapid microwave heating of the system was observed at higher electric field strength (0.5 V/Å) and high frequency of 500 GHz.
- A numerical relationship has been developed to predict the thermal response of bulk 3C-SiC system during microwave exposure at different electric field strengths and frequencies.
- The increased diffusion coefficient values from 5.11×10^{-4} Å^2/ns to 2.08 Å^2/ns for 5 ns of microwave heating revealed the physical phase change of 3C-SiC.
- At electric field strength of 0.5 V/Å (Phase II) and frequency of 500 GHz, the physical state of the system has changed by nearly 75% relative to the initial structure.

The outcomes of this study will support future efforts to design hybrid microwave heating setups for advanced material processing operations on metallic and non-metallic work materials.

Declaration of competing interest

The authors declare that they have no conflict of interests.

Acknowledgements

1. Tribeni Roy greatly acknowledges the financial support provided by the Science and Engineering Research Board (SERB), Government of India (SRG/2021/000741).
2. Saurav Goel acknowledge the financial support provided by the UKRI via Grants No. EP/S036180/1, EP/T001100/1 and EP/T024607/1, feasibility study awards to LSBU from the UKRI National Interdisciplinary Circular Economy Hub (EP/V029746/1) and Transforming the Foundation Industries: a Network+ (EP/V026402/1), the Hubert Curien Partnership award 2022 from the British Council, Transforming the Partnership award from the Royal Academy of Engineering (TSP1332) and the Newton Fellowship award from the Royal Society (NIF\R1\191571). This work also accessed the Isambard Bristol, UK supercomputing service via Resource Allocation Panel (RAP) as well as ARCHER2 resources (Project e648).
3. Hamed Yazdani Nezhad acknowledges the partially funding received from UK EPSRC on Self-Tuning Fibre-Reinforced Polymer Adaptive Nanocomposite (STRAINcomp), Ref. EP/R016828/1.

References

[1] R.R. Mishra, A.K. Sharma, Microwave-material interaction phenomena: Heating mechanisms, challenges and opportunities in material processing, Compos. Part A Appl. Sci. Manuf. 81 (2016) 78–97. https://doi.org/10.1016/j.compositesa.2015.10.035.

[2] D. Agrawal, Microwave sintering of ceramics, composites and metallic materials, and melting of glasses, Trans. Indian Ceram. Soc. 65 (2006) 129–144. https://doi.org/10.1080/0371750X.2006.11012292.

[3] D.E. Clark, W.H. Sutton, Microwave processing of materials, Annu. Rev. Mater. Sci. 26 (1996) 299–331. https://doi.org/10.1017/S0883769400038495.

[4] D. Li, J. Barrington, S. James, D. Ayre, M. Słoma, M.F. Lin, H. Yazdani Nezhad, Electromagnetic field controlled domain wall displacement for induced strain tailoring in BaTiO3-epoxy nanocomposite, Nature Publishing Group UK, 2022. https://doi.org/10.1038/s41598-022-11380-9.

[5] C.O. Mgbemena, D. Li, M.F. Lin, P.D. Liddel, K.B. Katnam, V.T. Kumar, H.Y. Nezhad, Accelerated microwave curing of fibre-reinforced thermoset polymer composites for structural applications: A review of scientific challenges, Compos. Part A Appl. Sci. Manuf. 115 (2018) 88–103. https://doi.org/10.1016/j.compositesa.2018.09.012.

[6] A.K. Sharma, R.R. Mishra, Role of particle size in microwave processing of metallic material systems, Mater. Sci. Technol. (United Kingdom). 34 (2018) 123–137. https://doi.org/10.1080/02670836.2017.1412043.

[7] S. Singh, D. Gupta, V. Jain, A.K. Sharma, Microwave processing of materials and applications in manufacturing industries: A Review, Mater. Manuf. Process. 30 (2015) 1–29. https://doi.org/10.1080/10426914.2014.952028.

[8] R. Krishnan, S.N. Shibu, D. Poelman, A.K. Badyal, A.K. Kunti, H.C. Swart, S.G. Menon, Recent advances in microwave synthesis for photoluminescence and photocatalysis, Mater. Today Commun. 32 (2022) 103890. https://doi.org/10.1016/j.mtcomm.2022.103890.

[9] R.R. Mishra, A.K. Sharma, A Review of Research Trends in Microwave Processing of Metal-Based Materials and Opportunities in Microwave Metal Casting, Crit. Rev. Solid State Mater. Sci. 41 (2016) 217–255. https://doi.org/10.1080/10408436.2016.1142421.

[10] E.T. Thostenson, T.W. Chou, Microwave processing: fundamentals and applications, Compos. Part A Appl. Sci. Manuf. 30 (1999) 1055–1071. https://doi.org/10.1016/S1359-835X(99)00020-2.

[11] D. El Khaled, N. Novas, J.A. Gazquez, F. Manzano-Agugliaro, Microwave dielectric heating: Applications on metals processing, Renew. Sustain. Energy Rev. 82 (2018) 2880–2892. https://doi.org/10.1016/j.rser.2017.10.043.

[12] Y. V Bykov, K.I. Rybakov, V.E. Semenov, High-temperature microwave processing of materials, J. Phys. D Appl. Phys. 34 (2001) R55–R75. https://doi.org/10.1016/0924-2244(96)81279-9.

[13] S.A.A. Alem, R. Latifi, S. Angizi, F. Hassanaghaei, M. Aghaahmadi, E. Ghasali, M. Rajabi, Microwave sintering of ceramic reinforced metal matrix composites and their properties: a review, Mater. Manuf. Process. 35 (2020) 303–327. https://doi.org/10.1080/10426914.2020.1718698.

[14] R.R. Mishra, A.K. Sharma, Effect of susceptor and mold material on microstructure of in-situ microwave casts of Al-Zn-Mg alloy, Mater. Des. 131 (2017) 428–440. https://doi.org/10.1016/j.matdes.2017.06.038.

[15] B. Yahaya, S. Izman, M. Konneh, N. Redzuan, Microwave Hybrid Heating of Materials Using Susceptors- A brief review, 845 (2014) 426–430. https://doi.org/10.4028/www.scientific.net/AMR.845.426.

[16] N.D. Afify, M.B. Sweatman, Classical molecular dynamics simulation of microwave heating of liquids: The case of water, J. Chem. Phys. 148 (2018). https://doi.org/10.1063/1.5001928.

[17] N.D. Afify, M.B. Sweatman, Molecular dynamics simulation of microwave heating of liquid monoethanolamine (MEA): An evaluation of existing force fields, J. Chem. Phys. 148 (2018). https://doi.org/10.1063/1.5022585.

[18] C. Wang, H. Liu, L. Song, J. Tan, W. Yang, L. Cheng, Temperature evolution, atomistic hot-spot effects and thermal runaway during microwave heating of polyacrylonitrile: A ReaxFF molecular dynamics simulation, Nano Sel. 2 (2021) 2373–2379. https://doi.org/10.1002/nano.202100061.

[19] Y. Hu, G. Jia, Molecular dynamics simulation investigation of the microwave heating supercritical water, J. Mol. Liq. 297 (2020) 111440. https://doi.org/10.1016/j.molliq.2019.111440.

[20] Y. Hu, A. Nakano, J. Wang, Directional melting of alumina via polarized microwave heating, Appl. Phys. Lett. 110 (2017). https://doi.org/10.1063/1.4973698.

[21] X. Yang, J. Zhang, S. Sagar, T. Dube, B.G. Kim, Y.G. Jung, D.D. Koo, A. Jones, J. Zhang, Molecular dynamics modeling of mechanical and tribological properties of additively manufactured AlCoCrFe high entropy alloy coating on aluminum substrate, Mater. Chem. Phys. 263 (2021) 124341. https://doi.org/10.1016/j.matchemphys.2021.124341.

[22] K.T. Chen, T.J. Wei, G.C. Li, M.Y. Chen, Y.S. Chen, S.W. Chang, H.W. Yen, C.S. Chen, Mechanical properties and deformation mechanisms in CoCrFeMnNi high entropy alloys: A molecular dynamics study, Mater. Chem. Phys. 271 (2021) 124912. https://doi.org/10.1016/j.matchemphys.2021.124912.

[23] A.P. Thompson, H.M. Aktulga, R. Berger, D.S. Bolintineanu, W.M. Brown, P.S. Crozier, P.J. in 't Veld, A. Kohlmeyer, S.G. Moore, T.D. Nguyen, R. Shan, M.J. Stevens, J. Tranchida, C. Trott, S.J. Plimpton, LAMMPS - a flexible simulation tool for particle-based materials modeling at the atomic, meso, and continuum scales, Comput. Phys. Commun. 271 (2022) 108171. https://doi.org/10.1016/j.cpc.2021.108171.

[24] T.A. Khan, P.A. Burr, D. Payne, M. Juhl, U. Das, B. Hallam, D. Bagnall, B. Puthen Veettil, Molecular dynamic simulation on temperature evolution of SiC under directional microwave radiation, J. Phys. Condens. Matter. 34 (2022). https://doi.org/10.1088/1361-648X/ac553c.

[25] M. Xu, Y.R. Girish, K.P. Rakesh, P. Wu, H.M. Manukumar, S.M. Byrappa, Udayabhanu, K. Byrappa, Recent advances and challenges in silicon carbide (SiC) ceramic nanoarchitectures and their applications, Mater. Today Commun. 28 (2021) 102533. https://doi.org/10.1016/j.mtcomm.2021.102533.

[26] A. Sarikov, A. Marzegalli, L. Barbisan, Molecular dynamics simulations of extended defects and their evolution in 3C – SiC by different potentials Molecular dynamics simulations of extended defects and their evolution in 3C – SiC by different potentials, Model. Simul. Mater. Sci. Eng. 28 (2020) Modelling and Simulation in Materials Science and. https://doi.org/https://doi.org/10.1088/1361-651X/ab50c7.

[27] J. Luo, A. Alateeqi, L. Liu, T. Sinno, Atomistic simulations of carbon diffusion and segregation in liquid silicon, 122 (2017) 225705.

[28] P. Vashishta, R.K. Kalia, A. Nakano, J.P. Rino, Interaction potential for silicon carbide : A molecular dynamics study of elastic constants and vibrational density of states for crystalline and amorphous silicon carbide Interaction potential for silicon carbide : A molecular dynamics study of elastic c, J. Appl. Phys. Phys. 101 (2007) 1–12. https://doi.org/10.1063/1.2724570.

[29] Y. Wu, B. Zou, L. Li, Molecular dynamics study on friction property between fused silica and SiC mold in high temperature molding, Mater. Today Commun. 26 (2021) 101878. https://doi.org/10.1016/j.mtcomm.2020.101878.

[30] pair_style vashishta command — LAMMPS documentation, (n.d.). https://docs.lammps.org/pair_vashishta.html (accessed August 19, 2022).

[31] D.J. Evans, B.L. Holian, The Nose-Hoover thermostat, J. Chem. Phys. 83 (1985) 4069–4074. https://doi.org/10.1063/1.449071.

[32] J. Cheng, R. Roy, D. Agrawal, Radically different effects on materials by separated microwave electric and magnetic fields, Mater. Res. Innov. 5 (2002) 170–177. https://doi.org/10.1007/s10019-002-8642-6.

[33] Y.M. Zhang, J.L. Li, J.P. Wang, X.S. Yang, B.Z. Wang, ReaxFF MDSs-based studies on gasification of glucose in supercritical water under microwave heating, Int. J. Hydrogen Energy. 41 (2016) 13390–13398. https://doi.org/10.1016/j.ijhydene.2016.05.158.

[34] P.S. Sokolov, V.A. Mukhanov, T. Chauveau, V.L. Solozhenko, On melting of silicon carbide under pressure, J. Superhard Mater. 34 (2012) 339–341. https://doi.org/10.3103/S1063457612050097.

[35] B. Aïssa, N. Tabet, M. Nedil, D. Therriault, F. Rosei, R. Nechache, Electromagnetic energy absorption potential and microwave heating capacity of SiC thin films in the 1-16 GHz frequency range, Appl. Surf. Sci. 258 (2012) 5482–5485. https://doi.org/10.1016/j.apsusc.2012.02.047.

[36] Y. Zhang, J. Li, X. Wang, J. Wang, B. Wang, Molecular Dynamics Simulation on

Temperature and Structure Characteristics of Microwave-Heating NaCI Solution, in: Int. Work. Microw. Millim. Wave Circuits Syst. Technol. Mol., IEEE, 2013: pp. 161–164.

[37] S. Chen, Y. Cheng, G. Zhang, Y.W. Zhang, Spontaneous directional motion of water molecules in single-walled carbon nanotubes with a stiffness gradient, Nanoscale Adv. 1 (2019) 1175–1180. https://doi.org/10.1039/c8na00322j.

[38] M. Chen, L. Hung, C. Huang, J. Xia, E.A. Carter, The melting point of lithium: An orbital-free first-principles molecular dynamics study, Mol. Phys. 111 (2013) 3448–3456. https://doi.org/10.1080/00268976.2013.828379.

[39] M.A. Vorontsova, P.G. Vekilov, D. Maes, Characterization of the diffusive dynamics of particles with time-dependent asymmetric microscopy intensity profiles †, Soft Matter. 12 (2016) 6926–6936. https://doi.org/10.1039/c6sm00946h.

[40] L. Weimann, K.A. Ganzinger, J. Mccoll, K.L. Irvine, S.J. Davis, A Quantitative Comparison of Single-Dye Tracking Analysis Tools Using Monte Carlo Simulations, PLoS One. 8 (2013) 64287. https://doi.org/10.1371/journal.pone.0064287.

[41] X. Li, X. Zhang, J. Chen, L. Huang, Y. Lv, The mechanical properties and creep behavior of epoxy polymer under the marine environment : A molecular dynamics investigation, Mater. Today Commun. 28 (2021) 102737. https://doi.org/10.1016/j.mtcomm.2021.102737.

[42] K. Vollmayr-Lee, Introduction to molecular dynamics simulations, Am. J. Phys. 88 (2020) 401–422. https://doi.org/10.1119/10.0000654.

[43] A. Owhal, D. Gautam, S.U. Belgamwar, V.K.P. Rao, Atomistic approach to analyse transportation of water nanodroplet through a vibrating nanochannel: scope in bio-NEMS applications, Mol. Simul. 48 (2022) 737–744. https://doi.org/10.1080/08927022.2022.2052065.

[44] N. V. Hong, N.T.T. Ha, H. V. Hung, M.T. Lan, P.K. Hung, Dynamics and diffusion mechanism in network forming liquid under high pressure: A new approach, Mater. Chem. Phys. 138 (2013) 154–161. https://doi.org/10.1016/j.matchemphys.2012.11.036.

[45] H.G. Abbas, J.R. Hahn, Crystallization mechanism of liquid tellurium from classical molecular dynamics simulation, Mater. Chem. Phys. 240 (2020) 122235. https://doi.org/10.1016/j.matchemphys.2019.122235.

[46] N. Farzi, F. Rahimi, H. Sabzyan, Proton conductivity of β-PCMOF2 in different temperatures and external electric fields: an insight from molecular dynamics simulation, Mater. Today Commun. 22 (2020) 100741. https://doi.org/10.1016/j.mtcomm.2019.100741.

[47] F. Chen, C. Cao, Q. Zhong, J. Liu, L. Yang, Z. Chen, Ab initio molecular dynamics study on local structure and dynamic properties of liquid Ni 62 Nb 38 alloy, Mater. Today Commun. 27 (2021) 102207. https://doi.org/10.1016/j.mtcomm.2021.102207.

[48] R. Tandon, A. Wereszczak, E. Lara-Curzio, Mechanical Properties and Performance of Engineering Ceramics II, John Wiley & Sons, Inc., Hoboken, NJ, USA, 2006. https://doi.org/10.1002/9780470291313.

[49] H. Sugawara, K. Kashimura, M. Hayashi, S. Ishihara, T. Mitani, N. Shinohara, Behavior of microwave-heated silicon carbide particles at frequencies of 2.0-13.5 GHz, Appl. Phys. Lett. 105 (2014) 0–5. https://doi.org/10.1063/1.4890849.